



Nuclear Science &
Technology Research Institute

Journal of Nuclear Research and Applications

Research Paper

Journal homepage: <http://jonra.nstri.ir>



Gamma Radiation Effects on the Mechanical Stability of Polyethylene Composites: Effects of Filler Dimension and Absorbed Dose

Z. Rafiei Sarmazdeh *

Nuclear Fuel Cycle Research School, Nuclear Science and Technology Research Institute, P.O. Box: 11365-8486, Tehran, Iran.

(Received: 24 August 2023, Revised: 3 December 2023, Accepted: 6 January 2024)

ABSTRACT

Incorporating multifunctional nanostructured materials that absorb radiation into polymers enhances their radiation-shielding properties. The role of boron nitride (BN) as an effective filler to enhance mechanical and shielding properties and resist irradiation has yet to be studied in detail. Our study examined the effects of gamma radiation doses ranging from 0 to 100 kGy on the mechanical properties of high-density polyethylene (HD) reinforced with two types of BN with different dimensions: hexagonal boron nitride (hBN) and boron nitride nanosheets (BNNSs). Scanning electron microscopy micrographs showed some aggregated plates with consistent distribution uniformly distributed in all regions in the matrix. This suggests proper adhesion between polyethylene and BN. The study showed that HD, 1 wt.% composite, and 1 wt.% nanocomposite samples experienced a 58%, 47%, and 33% reduction in elongation at break at 100 kGy compared to nonirradiated samples. The loss of tensile strength at 100 kGy for HD, 1 wt.% composite, and 1 wt.% nanocomposite was 57%, 44%, and 44%, respectively, compared to the nonirradiated samples. It is concluded that the addition of BNNSs in lower dimensions than hBN into polyethylene reduces the destructive effects of radiation. This is a way to improve the stability of polymer shields against ionizing radiation.

Keywords: Gamma, Irradiation, Composites, Mechanical property, Polyethylene, Boron nitride.

1. Introductions

With the increased usage of ionizing radiation in several scientific fields, there is a higher chance of severe injuries and health problems. These include radiation poisoning and burns. Therefore, it is now more crucial than ever to strictly control radiation [1-3].

People receive less radiation during radiation treatments reduced by adopting radiation protection techniques such as shielding in clinical oncology [4, 5]. Protecting humans and the environment from neutron and photon radiation (i.e., gamma and X-rays) is

* Corresponding Author E-mail: zrafiei@aeoi.org.ir

DOI: <https://doi.org/10.24200/jon.2024.1001>.

Further distribution of this work must maintain attribution to the author(s) and the published article's title, journal citation, and DOI.

essential when building a radiation plant. Research on radiation shielding is becoming increasingly interesting in polymer matrices and composites using filler/reinforcement. Numerous studies have been published on the creation of novel polymer composites based on boron compounds as ionizing radiation absorbers. [6-9].

Layered-boron-containing absorbers such as hexagonal boron nitride (h-BN) and boron nitride nanosheets (BNNs), as some of the most significant two-dimensional materials, are highly promising for thermal neutron shielding applications. This is due to their numerous exceptional physical, chemical, and mechanical properties, particularly their enormous thermal neutron capture cross-section (3840 barns for ^{10}B), which is several orders of magnitude larger than those of most other isotopes [10-13]. Currently, layered BN-containing composites are used in engineering and radiation shielding applications because they possess high strength, high elastic modulus, low weight, excellent resistance, etc. [14-18]. The mechanical properties of these composites depend on the matrix phase, dimension of reinforcement, distribution of reinforced particles in the matrix, and bonding between the matrix and reinforcement.

Research has suggested evaluating the radiation resistance of the proposed composites at various doses before making them commercially available [19]. Potential shielding materials may be defined by calculating several parameters. The most popular method for assessing a material's ability to operate as a shield is by analyzing the physical properties of samples subjected to radiation [6,20]. Researchers have shown that various properties of polymer composites are significantly influenced by gamma radiation. This is due to the type and size of the filler playing a crucial role. For instance, Bansel et al. reported that, especially at higher doses, gamma radiation improved the mechanical and

thermal characteristics of recycled low-density polyethylene biocomposites made of *Sesamum indicum* L. [21]. However, the addition of hydroxyapatite particles to PMMA composites resulted in a loss of mechanical characteristics, which were exacerbated by gamma radiation [22]. Hassan [23] says elongation at break decreases as talc content increases. In contrast, the tensile strength of gamma-irradiated waste polyethylene/recycled waste rubber powder (WPE/RWRP)/talc increases with talc content up to 10%. Additionally, with up to 50 kGy of irradiation, blend tensile strength increases, suggesting that crosslinking is the main mechanism. This team [24] also discovered that up to 20 wt.%, the physical characteristics of gamma-irradiated composites made of waste polyethylene (WPE), recovered waste rubber powder (RWRP), and glass fiber (GF) improved significantly with filler content. The enhancement of mechanical, thermal, and morphological characteristics may be attributed to the filler's reinforcement and the crosslinking caused by radiation. This is particularly at relatively mild levels of approximately 10 wt.% GF load and 75 kGy dosage. All of these investigations point to the complexity and diversity of gamma radiation's impact on polymer composite mechanical stability.

To the best of our knowledge, however, little research has been done on BN/PE's thermal, mechanical, and shielding characteristics [25-33]. There are very few reports on its radiation shielding performance. Shen, for instance, examined the impact of carbon-doped boron nitride (BCN) and modified BCN-KH550 on the mechanical, thermodynamic, and structural characteristics of silicon rubber composites both before and after γ irradiation [34]. The tensile strength and thermal characteristics of h-BN/epoxy resin composites were examined following γ -ray and neutron irradiation [35]. The radiation stability of hBN/HD and BNNs/HD composites exposed to

γ -rays is unknown, although their neutron shielding capabilities have been documented. There is still ongoing debate regarding the optimum filler dimensions and the underlying mechanisms governing this phenomenon. Further research is needed to fully understand the relationship between filler dimensions and mechanical stability.

Thus, an attempt was made to study the influence of the dimension of layered-BN materials on resisting irradiation stability and counter its deteriorating effects on polyethylene mechanical properties. In the current study, the typical mechanical properties of the gamma-irradiated hBN/HD composite and BNNSs/HD nanocomposite were evaluated using a tensile technique. To support the structural findings, scanning electron microscopy (SEM) studies were conducted to observe the morphological characteristics of the sample at two different BN-layered material concentrations.

2. Experimental

2.1 Materials

HBN (lateral dimensions 1 to 5 mm) was supplied by the Aldrich Company, and the BNNSs needed for the investigation were made using the method outlined in [36]. HD, called EX3 (Jam company, HM 5010 T2N, EX3), is employed.

2.2 Production of boron-containing composites and nanocomposites

Melt mixing was used to fabricate the hBN/HD composite and BNNSs/HD nanocomposite with a 1 wt.% filler component. The samples were produced at a processing temperature of 180 °C, a processing speed of 60 rpm, and a processing time of 10 min. First, the internal mixer was filled with high-density polyethylene. The system was loaded with layered-BN compounds when the torque stabilized for 90 seconds. The system

was blended for an additional 8.5 minutes. An HD sample was just put to melt mixing to compare the results. After the samples cooled, a hot press was used to produce the dumbbell-shaped samples needed for mechanical testing.

2.3 Characterization

The composite samples were created using an internal mixer (Brabender, Germany). Scanning electron microscopy (SEM) images were taken with a Hitachi S-4160 field emission SEM (FESEM) system to characterize the morphology of hBN and BNNSs. A Zeiss Evo18 SEM was also utilized to analyze the structural composition of the materials. For the microscopic examination of the HD/BN composite films, fracture surfaces were produced by breaking the samples after immersion in liquid nitrogen. Tensile test samples were irradiated to investigate the effect of ionizing radiation on mechanical properties. This was done in a gamma cell located in the Atomic Energy Organization of Iran. The source used was Co60 with an activity of 8775 Ci, and the samples were irradiated. The abrasive test based on the ASTM D638 standard was performed to determine the mechanical properties by the Hiwa/Material Testing, Hiwa-200 machine at a speed of 50 mm/min.

3. Results and discussion

Scanning electron microscopy is one of the most effective techniques for examining materials and polymer mixture morphology. Figure 1 (a,b) shows FESEM photographs of hBN and BNNSs. The image of hBN shows that, in accordance with the layered nature of hBN, the materials consist of thin particles or sheets. These particles or sheets have a lateral size between 1 and 5 mm and a thickness of over 50 nm [36]. BNNSs were also lamellar. At the same time, the BNNS sheets decreased and became more dispersed. Micrographs of HD fracture

surfaces reveal a uniform and continuous structure (Fig. 1 (c, d)).

To examine the structure and morphology of the composite samples at low and high magnification, SEM micrographs of the 1 wt.% composite and 1 wt.% nanocomposite are displayed (Figs. 2-3). Fig. As can be seen in Figure 2, hBN plates appear to have bright spots scattered over the dark HD substrate. The sample has a dispersed phase morphology in the continuous phase, and there are discrete hBN inclusions in a continuous matrix. These micrographs clearly show that hBN is available in a variety of sizes. The hBN plates in the composite matrix are well dispersed, parallel to each other, and perpendicular to the pressure

force of the hot-pressing stage of molding the sample [37]. The fracture surface of the hBN/HD composite is much rougher than that of the neat PE sample. This is probably due to the dispersion of filler platelets in the PE polymer matrix [37-39]. A high-magnification SEM micrograph of the composite shows hBN agglomeration composed of smaller particles or hBN platelets. Despite the agglomeration, the homogeneous distribution of hBN, which comprises some aggregated rather than BN sheets throughout the composites, indicates proper adhesion between polyethylene and boron nitride in the bulk. This is caused by the hydrophobic nature of the hBN surface.

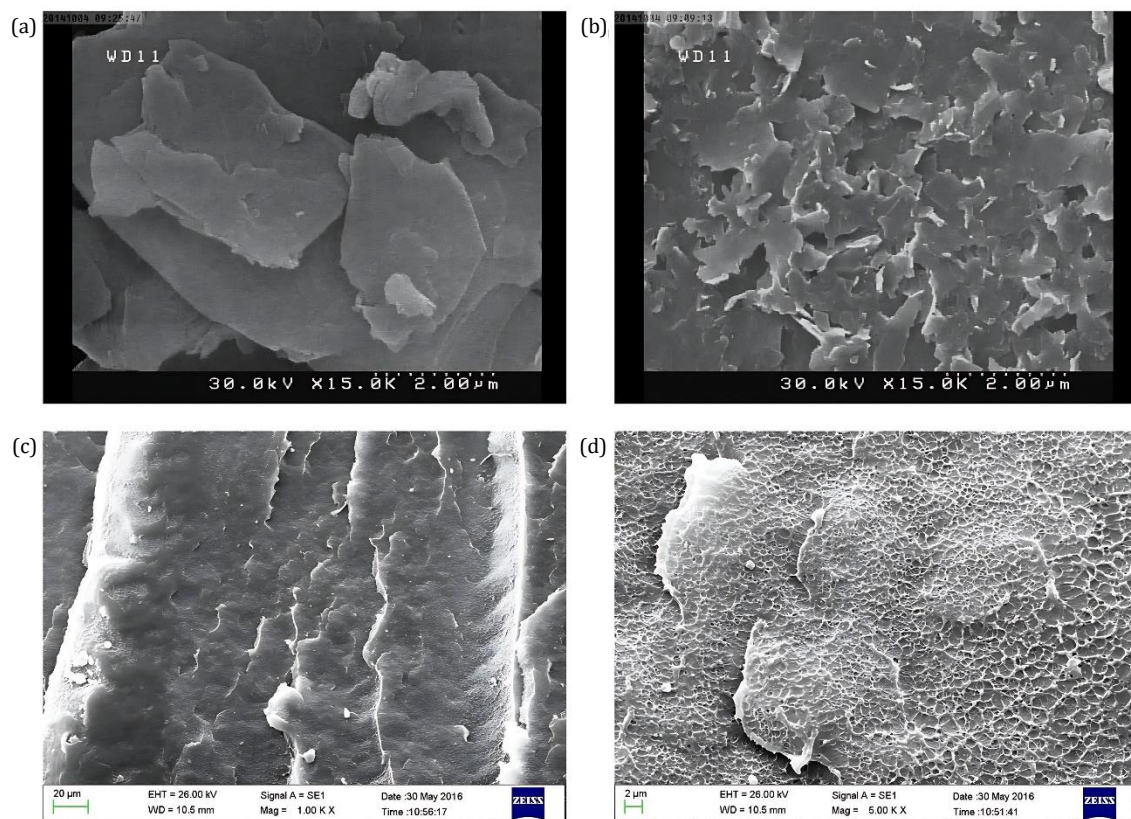


Fig. 1. SEM image of representative FESEM images of (a) the starting powder of h-BN and (b) BNNSs from h-BN precursors and SEM images of the neat HD fracture surface at (a) low and (b) high magnification.

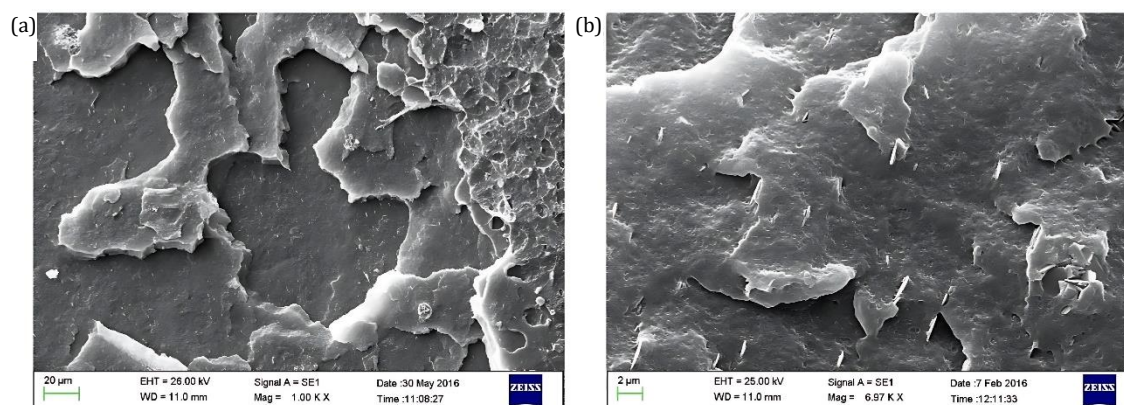


Fig. 2. SEM images of the composite fracture surface based on HD containing 1 wt.% hBN at (a) low and (b) high magnification.

SEM images of BNNSs/HD nanocomposites with 1 wt.% are shown in Fig. 3. The many dispersed nanosheets in the polyethylene substrate are visible at low magnification. However, the high magnification image of the nanocomposite reveals the aggregation of some of these nanosheets, making their thickness larger than the value stated in the production stage [36]. Additionally, a large accumulation of nanoplates can be seen on the left side of the image at high magnification. Nanosheets tend to minimize their contact surface with the polymer substrate due to the hydrophilic property of their surface [36] causes the aggregation and accumulation of these sheets.

To confirm the composite/nanocomposite structure, SEM combined with EDX mapping characterization was conducted. EDS mapping analysis was carried out on the selected region, which is shown as a pink rectangle in Fig. 4a, b. The analysis reveals elements such as boron, nitrogen, carbon, and oxygen. The blue dots, yellow dots, red dots, and green dots correspond to the distribution states of C, B, N, and O. This indicates that BN was successfully distributed into the polymer matrix [40] following the SEM results demonstrated in Fig. 2 and Fig. 3. In addition, EDX mapping disclosed the presence of oxygen, due to B2O3 contamination and BN materials often suffer from these contaminants [36, 41].

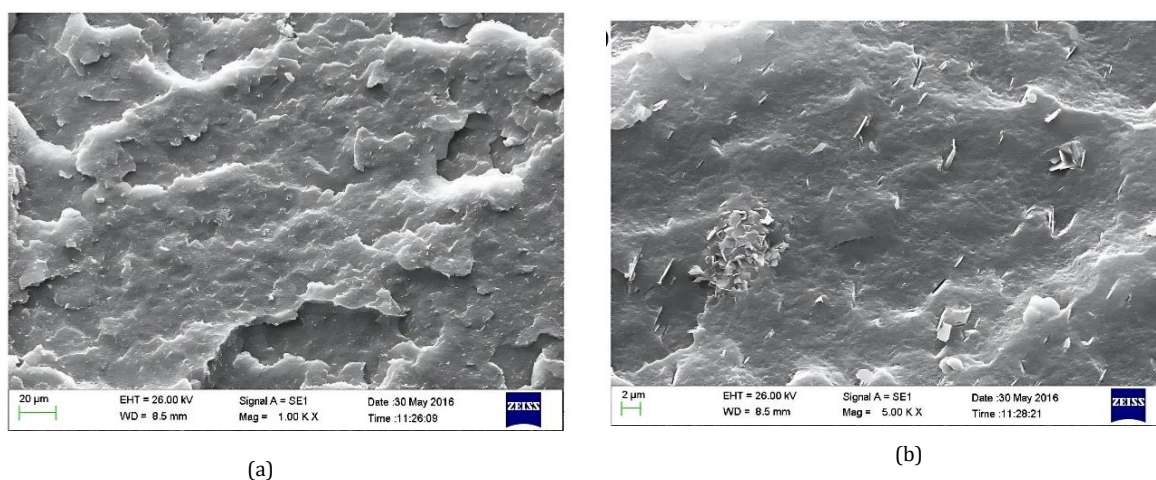


Fig. 3. SEM images of the nanocomposite fracture surface based on HD containing 1 wt.% BNNSs at (a) low and (b) high magnification.

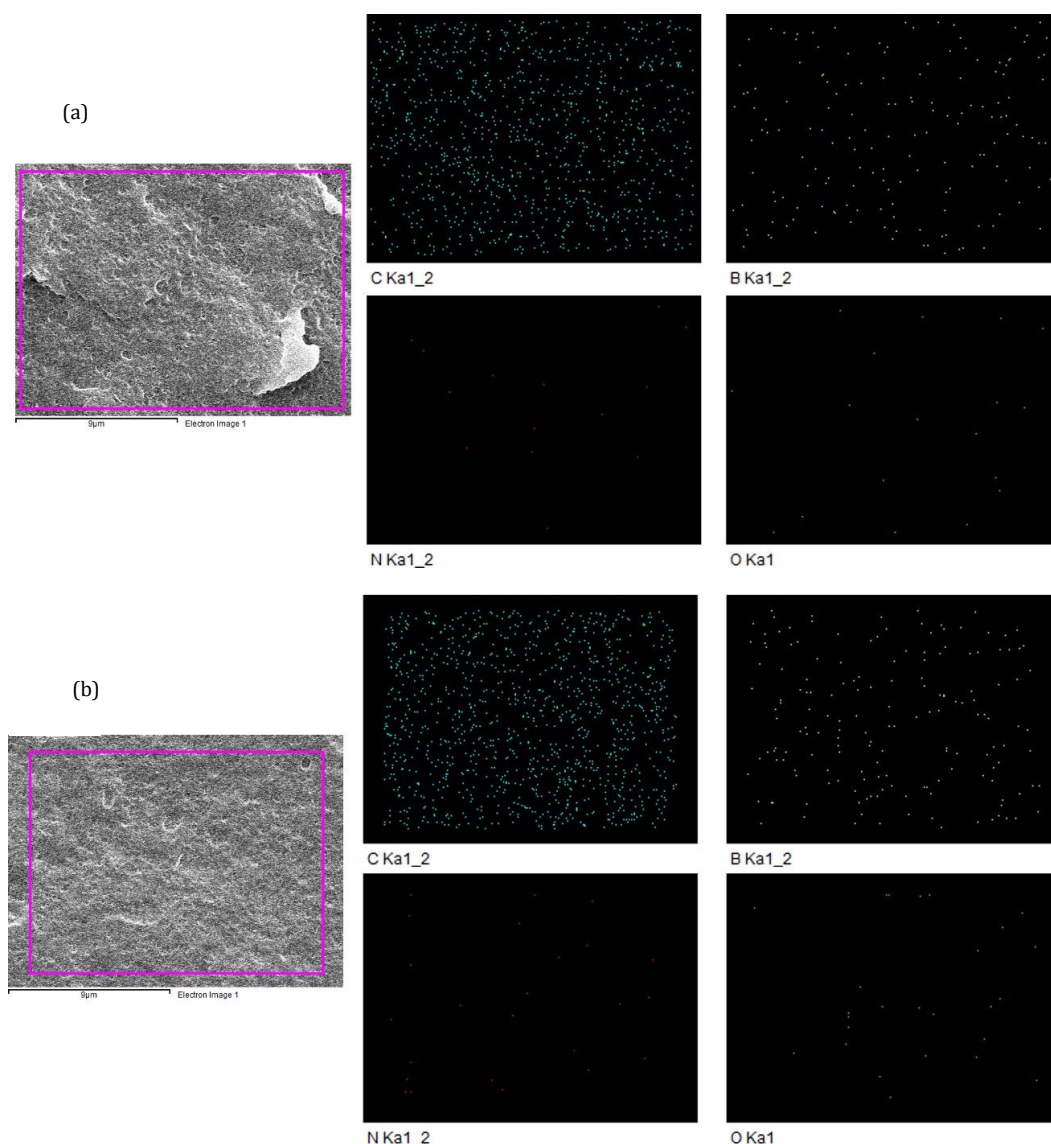


Fig. 4. SEM micrographs and elemental mapping of the hBN/HD composite (a) and (b) BNNSs/HD nanocomposite.

To further investigate the structure of the produced composites, an X-ray diffraction test was performed to investigate the influence of the boron nitride plates on the structure of polyethylene (Fig. 5). In the XRD pattern of hBN, the peaks at 26.72° and 41.59° correspond to interlayer spacings (calculated based on Bragg's law) of 3.33 \AA and 2.17 \AA , which correspond to the (002) and (100) planes, respectively [15, 36]. The nanosheet diffraction pattern shows significant changes compared to hBN. The sharp reduction in the peak intensity of the (002) plane and its shift to lower angles ($2\theta=26.66^\circ$) as well as the relative increase in FWHM

associated with Scherer broadening confirm the presence of exfoliated boron nitride nanosheets [36]. The HD diffraction pattern shows a strong peak at $2\theta=21.61^\circ$, a relatively strong peak at 23.96° , and a weak peak at 36.21° , which is related to the (110), (200), and (020) planes [15,42]. The characteristic BN peak of the hBN/HD composite has low intensity. Its FWHM increased from 0.28 to 0.47, while the (002) peak of BN in the BNNSs/HD nanocomposite disappeared. Structural characterization supports that the structure of the hBN/HD composite and BNNSs/HD nanocomposite is intercalated [43-45].

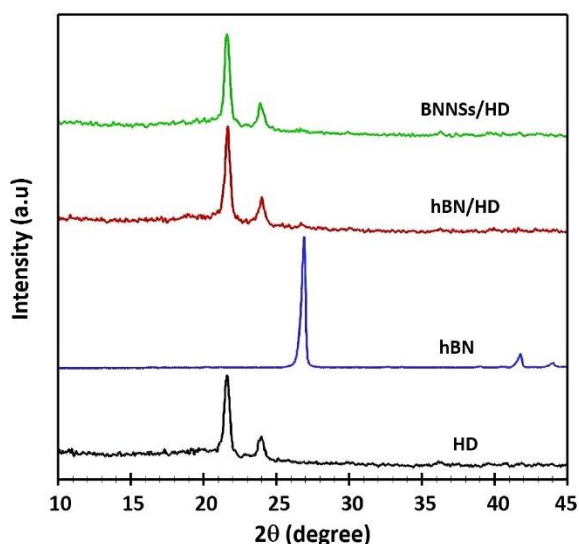


Fig. 5. XRD spectra of HD, hBN power, hBN/HD composite, and BNNSs/HD nanocomposite.

Three events occur when polyethylene samples are subjected to radiation: branching, chain scission, and cross-linking. Crosslinks, which improve mechanical properties, develop with random branching and chain scission, which hurt properties. The speed and quantity of these processes influence composite final behavior [46].

Singh provided two mechanisms for how irradiating polyethylene in air results in cross-linking and oxidative degradation in 1992 [47]. Radiation breaks the bond between carbon and hydrogen, producing radicals. These radicals combine with oxygen to form peroxides.



Since the rate of oxygen penetration is the limiting factor at high irradiation rates ($^3\text{103 Gy/s}$), reaction (1) is significant in competition with the other two processes, leading to a

dominant quantity of crosslink reactions. With a lower radiation rate, peroxide radicals formation and oxidative damage accelerate [47]. The prolonged irradiation time and low irradiation rate contribute significantly to the decreased strength of the material.

Fig. 6(a-c) shows the stress-strain diagrams of unirradiated and irradiated neat HD, 1 wt.% hBN/HD, and 1 wt.% BNNSs/HD at different dose levels. The peak stress and percentage of the strain of neat HD, composite, and nanocomposites decreased if the irradiation dose was increased. All materials, both nonirradiated and irradiated, exhibit hammering behavior; thus, well-known mechanical functions such as stretching, yielding, strain softening, cold stretching, and strain hardening are demonstrated in the stress-strain curves of the samples.

Tensile characteristics were taken from stress-strain diagrams of neat HD, hBN/HD composite, and BNNSs/HD nanocomposite at various doses to study the effects of layered-BN material dimension and absorbed dose on mechanical properties. In Figs. 7-9, the effects of the layered BN material dimensions and radiation dose on the tensile strength, Young's modulus, and elongation at break (El@Br) of neat HD, the composite, and the nanocomposite are displayed.

Tensile characteristics were taken from stress-strain diagrams of neat HD, hBN/HD composite, and BNNSs/HD nanocomposite at various doses to study the effects of layered-BN material dimension and absorbed dose on mechanical properties. In Figs. 7-9, the effects of the layered BN material dimensions and radiation dose on the tensile strength, Young's modulus, and elongation at break (El@Br) of neat HD, the composite, and the nanocomposite are displayed.

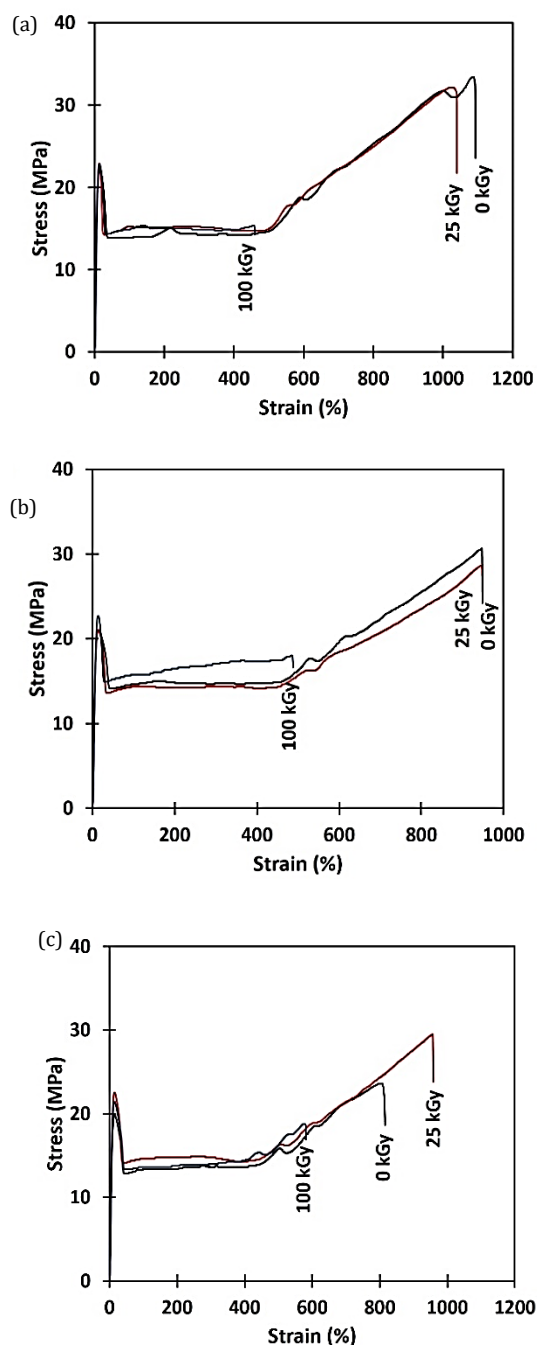


Fig. 6. Stress vs. strain diagrams of unirradiated and irradiated (a) neat HD (b) 1 wt.% hBN/HD composite and (c) 1 wt.% BNNSs/HD nanocomposite at different absorbed doses (0, 25, and 100 kGy).

The variations in modulus for neat HD and composites, including hBN and BNNSs, as a function of the absorbed dose of gamma radiation are shown in Figure 7. The Young's modulus of unirradiated neat HD and 1 wt.% composite and nanocomposite was 297.37, 313.05, and 353.01 MPa, respectively. Young's

modulus of the unirradiated hBN/HD and BNNSs/HD composites increased from 5.3% to 18.7% compared to that of neat HD with a change in the BN dimension. The corresponding values for a 100 kGy irradiation dose were 331.97, 327.65, and 302.91 MPa, respectively. The Young's modulus of neat HD increased by approximately 11.6%, that of the composite improved by 5%, and that of the nanocomposite was reduced by 14% when compared to the same unirradiated samples.

The modulus of neat HD and hBN/HD increases with increasing absorbed dose compared to unirradiated material. The HD matrix responds to irradiation by forming cross-link bonds, producing rigid areas that absorb loads and enhance modulus. The behavior of nanocomposites containing BNNSs is critical to consider because it exhibits a 14% drop in modulus with increasing dose, especially at 100 kGy, when compared to the sample not exposed to radiation. This characteristic most likely originates from the radiation resistance of nanosheets. The impact of radiation on the polyethylene matrix located between the sheets is reduced by boron nitride, which acts as a radiation barrier.

Due to the exfoliation of hBN, there are more BNNS sheets than hBN plates in equal composite contents, consistent with the comparison in Figs. 2 and 3. In the nanocomposite sample, the number of rigid (cross-linked) points decreases due to the large number of boron nitride plates, which act as a radiation barrier. Therefore, the cross-linking density between BN sheets is lower than the density outside these sheets. This leads to irregularities in the total density of the matrix, which increases the stress and ultimately reduces the modulus of the irradiated nanocomposite compared to the nonirradiated sample [48].

The tensile strength of the unirradiated 1 wt.% hBN/HD and 1 wt.% BNNSs/HD composites decreased from 11.2% to 8.9%

compared to that of neat HD with a change in BN dimension (Fig. 8). In the irradiated samples, the tensile strength decreased with increasing the absorbed dose. At 25 and 100 kGy, the decrease in tensile strength for the neat HD is 6.7 and 57.4%, respectively, compared to the unirradiated HD. The results show that the presence of layered-BN can reduce the amount of tensile strength reduction of irradiated samples so that the amount of tensile strength reduction at 25 and 100 kGy doses is 6.6% and 44% for composite and 3.3 and 44% for nanocomposite, respectively, compared to the unirradiated corresponding samples. Additionally, the effect of BNNSs on tensile strength at an absorbed dose of 25 kGy is greater than that of hBN.

For unirradiated samples, El@Br was reduced by 15.1% for composite materials and by 20.4% for nanocomposite materials compared to neat HD. It was also observed that the El@Br of the nanocomposite showed significantly higher values at 25 kGy than the unirradiated sample. With increasing radiation dose, the El@Br of nanocomposites increases up to 25 kGy and then decreases. This shows that cross-linking of the nanocomposite occurs after 25 kGy. At low doses, the uncross-connected nanocomposite acts as a plasticizer so that El@Br rises, while the nanocomposite exhibits a decrease in El@Br at a higher absorbed dose. This decline is due to cross-linked structures. At a high cross-link density, the network is so dense that the energy dissipation in the matrix is low and the energy supplied is used to break the bonds. At high cross-link density, the macromolecule segments become immobile, the system becomes stiffer and the elasticity decreases [49-53]. A higher radiation dose results in heightened crosslinking, which creates long-branched molecules with infinite mass and reduces chain mobility and stretching [54].

The role of BN nanosheets was assessed to compensate for mechanical loss. When compared to the corresponding unirradiated sample, the percentage reduction in tensile strength and El@Br of irradiated samples decreased as the BN dimension decreased. Additionally, it was shown that the high irradiation dose enhanced the percentage reduction in tensile strength and El@Br. It can be concluded that the mechanical property improvement of nanocomposites containing BNNSs with low dimensions and a low irradiation dose, compared to the neat polymer and composite, was substantial. BN nanosheets with smaller dimensions than hBN can improve the tensile parameters of HD composites because of the increased surface area. This results in a higher surface energy at the filler-matrix interface.

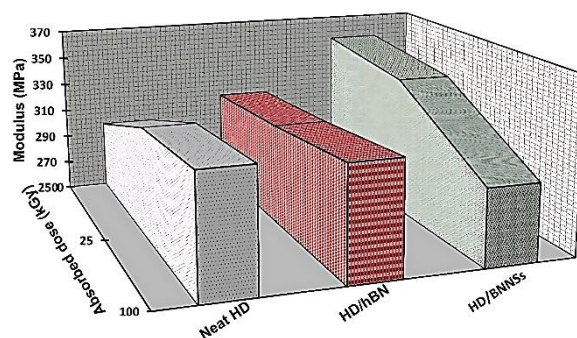


Fig. 7. Modulus of neat HD and HD composites (containing hBN and BNNSs) at different dimensions and irradiation dosages (0-100 kGy).

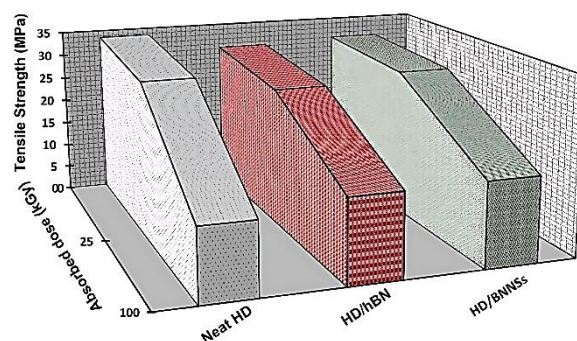


Fig. 8. Tensile strength of neat HD and HD composites (containing hBN and BNNSs) at different dimensions and irradiation doses (0-100 kGy).

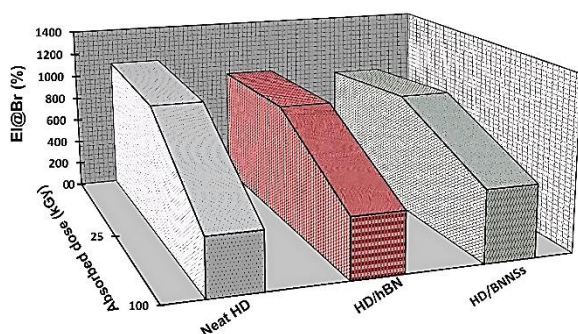


Fig. 9. EI@Br of neat HD and HD composites (containing hBN and BNNSs) at different dimensions and irradiation dosages (0-100 kGy).

4. Conclusions

High-density polyethylene was reinforced by hBN and BNNSs at 1 wt.% to form composites and nanocomposites. The prepared samples were gamma irradiated in air to study the effect of BN sheet dimensions on resisting problems due to irradiation. The studies mentioned above led to the following findings.

- The presence of BN sheets in the polyethylene matrix could effectively prevent mechanical property loss due to irradiation. This is more prominent at higher irradiation dosages.
- The addition of BN plates, particularly BNNSs, could restore polyethylene's ductile character at a higher irradiation dose.
- In samples with low-dimensional BN sheets and high irradiation doses, the property improvement of irradiated composites over neat polymers was quite considerable.

References

1. Almurayshid M, Helo Y, Kacperek A, Griffiths J, Hebden J, Gibson A. Quality assurance in proton beam therapy using a plastic scintillator and a commercially available digital camera. *J. Appl. Clin. Med. Phys.* 2017;18(5):210-219.
2. Almurayshid M, Alsagabi S, Alssalim Y, Alotaibi Z, Almsalam R. Feasibility of polymer-based composite materials as radiation shield. *Radiat. Phys. Chem.* 2021;183:109425-109432.
3. Ryan JL. Ionizing radiation: the good, the bad, and the ugly. *J. Invest. Dermatol.* 2012;132:985-993.
4. Salehi D, Sardari D, Jozani MS. Investigation of some radiation shielding parameters in soft tissue. *Radiat. Res. Appl. Sci.* 2015;8(3):439-445.
5. Ferrari C, Manenti G, Malizia A. Sievert or Gray: Dose Quantities and Protection Levels in Emergency *Exposure. Sensors.* 2023;23(4):1918-1927.
6. Shahzad K, Kausar A, Manzoor S, Rakha SA, Uzair A, Sajid M, et al. Views on Radiation Shielding Efficiency of Polymeric Composites/Nanocomposites and Multi-Layered Materials: Current State and Advancements. *Radiation.* 2023;3(1):1-20.
7. More CV, Alsayed Z, Badawi MS, Thabet AA, Pawar PP. Polymeric composite materials for radiation shielding: a review. *Environ. Chem. Lett.* 2021;19(3):2057-2090.
8. Almuqrin AH, Alasali HJ, Sayyed MI, Mahmoud KG. Preparation and experimental estimation of radiation shielding properties of novel epoxy reinforced with Sb₂O₃ and PbO. *E-Polym.* 2023;23(1):20230019-20230028.
9. Elsafi M, El-Nahal MA, Sayyed MI, Saleh IH, Abbas MI. Novel 3-D printed radiation shielding materials embedded with bulk and nanoparticles of bismuth. *Sci. Rep.* 2022;12(1):12467-12476.
10. Doan TC, Majety S, Grenadier S, Li J, Lin JY, Jiang HX. Hexagonal boron nitride thin film thermal neutron detectors with high energy resolution of the reaction products. *Nucl. Instrum. Methods Phys. Res. A.* 2015;783:121-127.
11. Chetverikov YO, Bykov AA, Krotov AV, Mistonov AA, Murashev MM, Smirnov IV, et al. Boron-containing plastic composites as neutron shielding material for additive manufacturing processes. *Nucl. Instrum. Methods Phys. Res. A.* 2023;1055:168406-168412.
12. Dong M, Zhou S, Xue X, Feng X, Sayyed MI, Khandaker MU, et al. The potential use of boron containing resources for protection against nuclear radiation. *Radiat. Phys. Chem.* 2021;188:109601-109610.
13. Qi Z, Yang Z, Li J, Guo Y, Yang G, Yu Y, et al. The Advancement of Neutron-Shielding Materials for the Transportation and Storage of Spent Nuclear Fuel. *Mater.* 2022;15(9):3255-3278.
14. Shin JW, Lee J-W, Yu S, Baek BK, Hong JP, Seo Y, et al. Polyethylene/boron-containing composites for radiation shielding. *Thermochim. Acta.* 2014;585:5-9.
15. Shang Y, Yang G, Su F, Feng Y, Ji Y, Liu D, et al. Multilayer polyethylene/ hexagonal boron nitride composites showing high neutron

- shielding efficiency and thermal conductivity. *Compos. Commun.* 2020; 19:147-153.
16. Harrison C, Weaver S, Bertelsen C, Burgett E, Hertel N, Grulke E. Polyethylene/boron nitride composites for space radiation shielding. *J. Appl. Polym. Sci.* 2008; 109(4):2529-2538.
 17. Zaccardi F, Toto E, Rastogi S, La Saponara V, Santonicola MG, Laurenzi S. Impact of Proton Irradiation on Medium Density Polyethylene/Carbon Nanocomposites for Space Shielding Applications. *Nanomater.* 2023;13(7):1288-1304.
 18. Uddin Z, Yasin T, Shafiq M, Raza A, Zahur A. On the physical, chemical, and neutron shielding properties of polyethylene/boron carbide composites. *Radiat. Phys. Chem.* 2020;166:108450-108457.
 19. Mirji R, Lobo B, editors. 24. Radiation shielding materials: A brief review on methods, scope and significance. *Proc. Nation. Conf. 'Advances in VLSI and Microelectronics*;2017:96-100.
 20. Naito M, Kitamura H, Koike M, Kusano H, Kusumoto T, Uchihori Y, et al. Applicability of composite materials for space radiation shielding of spacecraft. *Life. Sci. Space. Res.* 2021;31:71-79.
 21. Bansal N, Ahuja S, Lal S, Arora S. Agricultural-waste Sesamum indicum L./recycled-low density polyethylene bio-composites: Impact of gamma radiation on mechanical and thermal properties. *J. Reinf. Plast. Compos.* 2023;0(0):1-16.
 22. Albano C, Karam A, Gonzalez G, Domínguez N, Sanchez YJMC, Crystals L. Study of gamma radiation effect on PMMA/HA composites prepared by solution. *Mol. Cryst. Liq.* 2006;448(1):243-249.
 23. Hassan MM, Aly RO, Hasanen JA, El Sayed ESF. Influence of talc content on some properties of gamma irradiated composites of polyethylene and recycled rubber wastes. *J. Appl. Polym. Sci.* 2010;117(4):2428-2435.
 24. Hassan MM, Aly RO, Hasanen JA, El Sayed FJJoI, Chemistry E. The effect of gamma irradiation on mechanical, thermal and morphological properties of glass fiber reinforced polyethylene waste/reclaim rubber composites. *J. Ind. Eng. Chem.* 2014;20(3):947-952.
 25. Herrman K, Baxter LN, Mishra K, Benton E, Singh RP, Vaidyanathan RK. Mechanical characterization of polyethylene-based thermoplastic composite materials for radiation shielding. *Comp. Commun.* 2019;13:37-41.
 26. Herrman k. Mechanical and radiation shielding properties of boron nitride reinforced high-density polyethylene. (*Doctoral dissertation, Oklahoma State University*);2020.
 27. Harrison C, Burgett E, Hertel N, Grulke E. Polyethylene/Boron Composites for Radiation Shielding Applications. *AIP Conf. Proc.* 2008;969(1):484-491.
 28. Harrison C, Burgett E, Hertel N, Grulke E. Polyethylene/Boron Containing Composites for Radiation Shielding Applications. *Nanostructured Materials and Nanotechnology II: Ceramic Engineering and Science Proceedings*, 2009;29:77-84.
 29. Cinan ZM, Erol B, Baskan T, Mutlu S, Ortaç B, Savaskan Yilmaz S, et al. Radiation Shielding Tests of Crosslinked Polystyrene-b-Polyethyleneglycol Block Copolymers Blended with Nanostructured Selenium Dioxide and Boron Nitride Particles. *Nanomater.* 2022;12(3):297-327.
 30. Jamali F, Mortazavi SMJ, Kardan M, Mosleh-Shirazi MA, Sina S, Rahpeyma J. Developing light nano-composites with improved mechanical properties for neutron shielding. *Kerntechnik.* 2017;82(6):648-652.
 31. İrim ŞG, Wis AA, Keskin MA, Baykara O, Ozkoc G, Avci A, et al. Physical, mechanical and neutron shielding properties of h-BN/Gd₂O₃/HDPE ternary nanocomposites. *Radiat. Phys. Chem.* 2018;144:434-443.
 32. Vira AD, Mone EM, Ryan EA, Connolly PT, Smith K, Roecker CD, et al. Designing a boron nitride polyethylene composite for shielding neutrons. *APL Mater.* 2023;11:101104-101115.
 33. Zhang W, Feng Y, Althakafy JT, Liu Y, Abo-Dief HM, Huang M, et al. Ultrahigh molecular weight polyethylene fiber/boron nitride composites with high neutron shielding efficiency and mechanical performance. *Adv. Compos. Hybrid Mater.* 2022;5(3):2012-2020.
 34. Shen H, Wu Z, Dou R, Jiao L, Chen G, Lin M, et al. The effect of modified carbon-doped boron nitride on the mechanical, thermal and γ -radiation stability of silicone rubber composites. *Polym. Degrad. Stab.* 2023;218:110542-110549.
 35. Jiao L, Wang Y, Wu Z, Shen H, Weng H, Chen H, et al. Effect of gamma and neutron irradiation on properties of boron nitride/epoxy resin composites. *Polym. Degrad. Stab.* 2021;190:109643-109667.
 36. Rafiei-Sarmazdeh Z, Jafari SH, Ahmadi SJ, Zahedi-Dizaji SM. Large-scale exfoliation of hexagonal boron nitride with combined fast quenching and liquid exfoliation strategies. *J. Mater. Sci.* 2016;51(6):3162-3169.
 37. Wang Z, Priego P, Meziani MJ, Wirth K, Bhattacharya S, Rao A, et al. Dispersion of high-quality boron nitride nanosheets in polyethylene for nanocomposites of superior thermal transport properties. *Nanoscale Adv.* 2020;2(6):2507-2513.
 38. Zhi Y-R, Yu B, Yuen ACY, Liang J, Wang L-Q, Yang W, et al. Surface Manipulation of Thermal-Exfoliated Hexagonal Boron Nitride with

- Polyaniline for Improving Thermal Stability and Fire Safety Performance of Polymeric Materials. *ACS Omega*. 2018;3(11):14942-14952.
39. Ajayi AA, Turup Pandurangan M, Kanny K. Influence of hybridizing fillers on mechanical properties of foam composite panel. *Polym. Eng. Sci.* 2023;63(8):2565-2577.
 40. Jiang X, Ma P, You F, Yao C, Yao J, Liu F. A facile strategy for modifying boron nitride and enhancing its effect on the thermal conductivity of polypropylene/polystyrene blends. *RSC Adv.* 2018;8(56):32132-32137.
 41. Štengl V, Henych J, Kormunda MJSAM. Self-assembled BN and BCN quantum dots obtained from high intensity ultrasound exfoliated nanosheets. *Sci. Adv. Mater.* 2014;6(6):1106-1116.
 42. Okan BS. Fabrication of multilayer graphene oxide-reinforced high density polyethylene nanocomposites with enhanced thermal and mechanical properties via thermokinetic mixing. *Turk. J. Chem.* 2017;41:381-390.
 43. Guo Y, Peng F, Wang H, Huang F, Meng F, Hui D, et al. Intercalation Polymerization Approach for Preparing Graphene/Polymer Composites. *Polym.* 2018;10(1):61-88.
 44. Block KA, Trusiak A, Katz A, Alimova A, Wei H, Gottlieb P, et al. Exfoliation and intercalation of montmorillonite by small peptides. *Appl. Clay Sci.* 2015;107:173-181.
 45. Wang N. Flame Retardancy of Polymer Nanocomposites based on Layered Aluminum Phosphate and Computational Study of Intercalation of Amines into α -Zirconium Phosphate and Adsorption of a Model Organic Pollutant. *Milwaukee, Wisconsin:Marquette University*;2011.
 46. Cota SS, Vasconcelos V, Senne Junior M, Carvalho LL, Rezende DB, Correa RF. Changes in mechanical properties due to gamma irradiation of high-density polyethylene (HDPE). *Braz. J. Chem. Eng.* 2007;24(2):259-265.
 47. Singh A. Irradiation of polyethylene:Some aspects of crosslinking and oxidative degradation. *Rad. Phys. Chem.* 1999;56(4):375-380.
 48. Elsharkawy ER, Hegazi EM, Abd El-megeed AJJMCP. Effect of gamma irradiation on the structural and properties of high density polyethylene (HDPE). *Int. J. Mater. Chem. Phys.* 2015;1:384-387.
 49. Hassan MM, El-Nemr KF, El-Megeed AAA. Effect of gamma radiation on physico-mechanical properties of vulcanized natural rubber/carbon fiber composites. *J. Elastomers Plast.* 2015;48(8):677-690.
 50. Khozemy EE, Radi H, Mazied NA. Upcycling of waste polyethylene and cement kiln dust to produce polymeric composite sheets using gamma irradiation. *Polym. Bull.* 2023;80(5):5183-5201.
 51. Hassan MM, Aly RO, El-Ghandour AH, Abdelnaby HA. Effect of gamma irradiation on some properties of reclaimed rubber/nitrile-butadiene rubber blend and its swelling in motor and brake oils. *J. Elastomers Plast.* 2012;45(1):77-94.
 52. Yasin T, Khan S, Nho Y-C, Ahmad R. Effect of polyfunctional monomers on properties of radiation crosslinked EPDM/waste tire dust blend. *Radiat. Phys. Chem.* 2012;81(4):421-425.
 53. Ali MA, El-Nemr KF, Hassan MM. Waste newsprint fibers for reinforcement of radiation-cured styrene butadiene rubber-based composites - Part I:Mechanical and physical properties. *J. Reinf. Plast. Compos.* 2011;30(8):721-737.
 54. Krashennnikov AV, Nordlund K. Irradiation effects in carbon nanotubes. *Nucl. Instrum. Methods Phys. Res. B.* 2004;216:355-366.

How to cite this article

Z. Rafiei Sarmazdeh, *Gamma Radiation Effects on the Mechanical Stability of Polyethylene Composites: Effects of Filler Dimension and Absorbed Dose*, Journal of Nuclear Science and Applications (JONRA) Volume 4 Number 1 Winter (2024) 12-22.
 URL: https://jonra.nstria.ir/article_1622.html, DOI: <https://doi.org/10.24200/jon.2024.1001>.



This work is licensed under the Creative Commons Attribution 4.0 International License.
 To view a copy of this license, visit <http://creativecommons.org/licenses/by/4.0>